THE JOURNAL OF PHYSICAL CHEMISTRY B
A JOURNAL OF THE AMERICAN CHEMICAL SOCIETY

pubs.acs.org/JPCB

Article

Crustwater: Modeling Hydrophobic Solvation

Published as part of The Journal of Physical Chemistry virtual special issue "Pablo G. Debenedetti Festschrift".

Ajeet Kumar Yadav, Pradipta Bandyopadhyay, Evangelos A. Coutsias, and Ken A. Dill*

Cite This: https://doi.org/10.1021/acs.jpcb.2c02695

Read Online

ACCESS | Metrics & More | Article Recommendations | Supporting Information

ABSTRACT: We describe Crustwater, a statistical mechanical model of nonpolar solvation in water. It treats bulk water using the Cage Water model and introduces a *crust*, i.e., a solvation shell of coordinated partially structured waters. Crustwater is analytical and fast to compute. We compute here solvation vs temperature over the liquid range, and vs pressure and solute size. Its thermal predictions are as accurate as much more costly explicit models such as TIP4P/2005. This modeling gives new insights into the hydrophobic effect: (1) that oil−water insolubility in cold water is due to solute−water (SW) translational entropy and not water−water (WW) orientations, even while hot water is dominated by WW cage breaking, and (2) that a size transition at the Angstrom scale, not the nanometer scale, takes place as previously predicted.

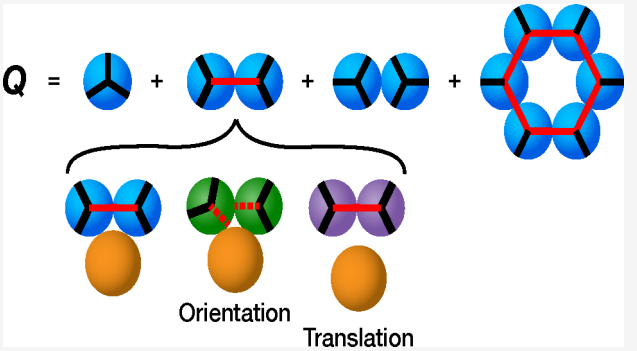

Downloaded via 67.0.84.132 on August 6, 2022 at 15:12:40 (UTC).
See https://pubs.acs.org/sharingguidelines for options on how to legitimately share published articles.

INTRODUCTION

Molecules and materials in water are often studied by computational molecular physics. Such modeling would benefit from improving upon either today's explicit or implicit water models. On the one hand, there is a need for modeling, like explicit water often is, that is transferable across systems beyond the parametrized domain, that captures the essential atomistic physics faithfully, and that is accurate enough to reproduce experiments.[1−8] On the other hand, the benefit of implicit water is its high computational efficiency, particularly for treating large, slow complex systems. But, the trade-off between explicit and implicit is quite drastic. For example, the solvation shell is either treated as atomistic water molecules that are sampled stochastically or treated as a simple continuum having no water structure at all.

In the present work, we offer a third option that makes a different trade-off. Here, we treat the solvation shell as having tetrahedral waters, treated through statistical mechanical averaging and combined with a surface physics term. Perhaps the following terminology helps clarify our objective. Explicit refers to Particulatewaters that are sampled individually over very many microstates. Implicit refers to Smearedwater that is a continuum with no structure. We call the present model *Crustwater* because solvation entails a "crust" of a relatively small number of mesostates of water−water arrangements of first-shell waters that can be enumerated by statistical mechanical averaging.

Crustwater is largely analytical, so it is very fast to compute, is not subject to the errors and fluctuations of trajectory simulations, gives physically interpretable results, and gives explicit dependences on temperature, pressure, and solute radius for simple spherical solutes. One key result here is an exact analytical expression for distributions of tetrahedral water conformations around a sphere. What the present approach trades off is some degree of transferability because of the simple approximate nature of our surface physics term.

As a starting point toward more complex solutes, we treat here the hydrophobic effect of small spherical solutes. Ever since the work of Frank and Evans in 1945,[9] there has been interest in understanding the structural physical basis of the hydrophobic effect,[10−13] i.e., of nonpolar solvation in water, including its volumetric and energetic anomalies. Accurate models of aqueous solvation of nonpolar solutes are needed to predict properties of proteins, membranes, and nucleic acids, in their folding, ligand binding, complexation and assemblies, and interactions with surfaces,[12,14−19] as well as to engineer and design materials that can filter clean water, and to understand earth's geochemistry and hydrological cycles.[11]

We treat here the inert gases and roughly spherical molecular solutes—methane, benzene, naphthalene, and fullerene. We find that the dependences of solvation free energy, enthalpy, entropy and heat capacity on temperature and solute radius are roughly as accurate as in SPC and TIP explicit water

Received: April 19, 2022
Revised: July 13, 2022

ACS Publications

© XXXX The Authors. Published by American Chemical Society

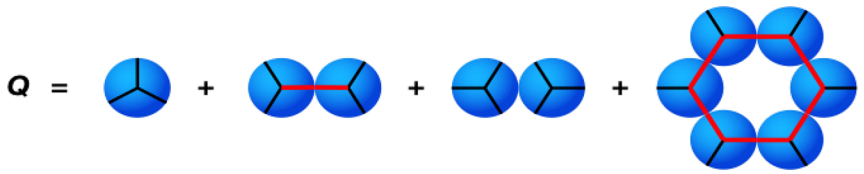

Figure 1. Cage Water partition function for pure water. It has four components: one for noncontacting water molecules, one for H-bonding water pairs, one for LJ pairs, and one for cage-like structures (from left to right); red lines represent hydrogen bonds. The model is 3D; this 2D picture is just for illustration.

simulations of Paschek[5] and Dyer et al.[20] In addition, we predict pressure dependences.

METHODOLOGY

We start with the Cage Water model of pure water,[21] which captures the combined symmetries of tetrahedral cage-like hydrogen-bonding structures and radial van der Waals forces using a fast-to-compute statistical physical partition function. It predicts experimental data on pure liquid water roughly equivalent to that of the TIP4P/2005[22] simulational model, but much faster than simulations since Cage Water is essentially analytical. Into the Cage Water model, we introduce small spherical nonpolar solutes. This solvation step entails primarily four components: an enthalpy of the solute−water interaction, water−water enthalpy and entropy, an orientational entropy geometric restriction of first-shell water−water hydrogen bonding, and a translational entropy restriction that depends on the strength of the solute−water interaction.

Treating the Pure Liquid Using the Cage Water Model (without Solute). We start from the Cage Water model of pure liquid water[21] called Cage Water. It develops a statistical mechanical partition function for four types of states: isolated individual waters, pairs of hydrogen-bonded (H-bonded) waters, Lennard-Jones (LJ) pairs (having no hydrogen bonds), and H-bonded water cages that resemble those inside ice I_h. Here, we have used 6-membered-water cages.[23,24] Figure 1 illustrates these terms with a cartoon. The partition function of a hexagonal cage of water molecules is given in eq 1. (The definitions and the expressions for each state are given in the Supporting Information.)

$$Q_1 = (\Delta_{HB} + \Delta_{LJ} + \Delta_O)^6 - {\Delta_{HB}}^6 + e^{(-\beta\epsilon_c)}{\Delta_{cage}}^6 \quad (1)$$

where Δ_{HB}, Δ_{LJ}, and Δ_O are the partition functions of a pairwise H-bonded state and LJ and open states, respectively. Δ_{cage} is the partition function of a cooperative H-bonded state, termed as cage, and ϵ_c is the cooperativity energy that comes into the picture only when all six molecules of the hexagon are H-bonded to make a full hexagonal cage.[23,24] From the partition function, we can compute all thermodynamic properties such as isothermal compressibility, coefficient of thermal expansion, the fractional population of each state, the molar volume, specific heat etc. In the following, we first give the general expression for the hydration free energy, followed by the description of the effect of solute insertion on the first solvation shell waters.

Estimating the Solvation Free Energy. The free energy of solvation (ΔG) in terms of total partition function of pure water and the water−solute system is given as

$$\Delta G = -kT \ln \frac{Q_h}{Q_b} \quad (2)$$

where k, T, Q_h and Q_b are the Boltzmann constant, temperature, and the total partition function of water with solute (h, for hydration) and without solute (b, for bulk), respectively. Equation 2 can be simplified by considering that, in our model of solvation, solute affects only the first solvation shell of waters. Hence, in our model, the partition function of the waters, not in the hydration shell, is same with and without the solute. Equations 3 and 4 show the partition function after cancellation of the partition functions of the nonhydration waters. Here, q_b and q_h denote the partition function of an average water without and with the solute, respectively; $n(r)$ being the number of waters in the solvation shell that depends on the radius of the solute r.[25]

$$\Delta G = -kT \ln \frac{{q_h}^{n(r)}}{{q_b}^{n(r)}} \quad (3)$$

$$\Delta G = -n(r)kT \ln \frac{q_h}{q_b} \quad (4)$$

Now the task is to calculate q_b and q_h. This is done by using the average energy of one water molecule with and without the solute, denoted by $\langle \varepsilon(\zeta(\theta_0))\rangle_h$ and $\langle \epsilon\rangle_b$ respectively where $\zeta(\theta_0)$ is the average number of HBs per water (ranging from 0 to 4), with θ_0 being the critical angle defined in the Supporting Information (see Figure S2). Then the partition functions are calculated using eqs 5 and 6, where p, $v_{mol,i}$ are the pressure and molar volume ($i = b$ and h denote bulk water and water with a solute, respectively), respectively.

$$q_b = \iint d\phi\, d\psi \int_0^{\pi/3} \sin(\theta) \exp\left(-\frac{\langle \epsilon\rangle_b + pv_{mol,b}}{kT}\right) d\theta \quad (5)$$

$$q_h = \iint d\phi\, d\psi \int_0^{\pi/3} \sin(\theta) \exp\left(-\frac{\langle \epsilon(\zeta(\theta_0))\rangle_h + pv_{mol,h}}{kT}\right) d\theta \quad (6)$$

where θ, ϕ, and ψ are the Euler angles. The expressions for the average energies are, for hydration shell water (see the Supporting Information, eq S19):

$$\langle \epsilon(\zeta(\theta_0))\rangle_h = \frac{1}{2}[\langle \zeta(\theta_0)\rangle\{\langle u_{HB}\rangle f_{HB} + \langle u_{cage}\rangle f_{cage}\} + 4\langle u_{LJ}\rangle f_{LJ} + \epsilon_{SW}] \quad (7)$$

and for bulk water (see the Supporting Information, eq S4):

$$\langle \epsilon\rangle_b = 2[\langle u_{HB}\rangle f_{HB} + \langle u_{cage}\rangle f_{cage} + \langle u_{LJ}\rangle f_{LJ}] \quad (8)$$

where $\langle u_i\rangle$'s and f_i's are the average energies and fractional populations of the states, respectively (calculated in the same

https://doi.org/10.1021/acs.jpcb.2c02695
J. Phys. Chem. B XXXX, XXX, XXX−XXX

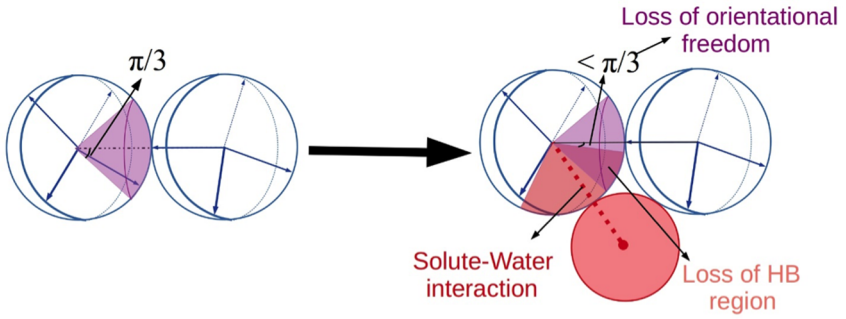

Figure 2. Inserting a solute imposes geometric restrictions on first-shell H-bonding waters. Solute insertion does two things: (a) it can reduce the hydrogen bonding between waters and the orientational freedom of waters, and (b) it introduces a solute−water interaction.

way as in refs 23−25), and ϵ_{SW} is the solute−water interaction energy.

Here is our modeling procedure. First, for pure bulk water, as previously described in the Cage Water model,[21] we start from the water−water energies − HB, LJ, and cooperativity c− then, integrate over all the possible configurations to get q_b. (The other thermodynamic properties of pure water follow directly—the heat capacities, enthalpies, free energies and volumes of pure water's liquid states—by using standard thermodynamic relations.) Second, insertion of a spherical solute molecule perturbs the water molecules in the first solvation shell. Often, in earlier conceptions of the hydrophobic effect, solute insertion was assumed to simply introduce an energy of interaction of the solute with first-shell waters. It was assumed that the unusual temperature dependence of nonpolar solvation could all be attributed just to bulk water itself. But, here we adopt a different approach. In particular, the success of the Cage Water approach in predicting the thermal and volumetric properties leads us to trust its microscopic physical basis as a good starting model for now treating solvation.

The paragraphs below describe how we divide the solvation step into two components: (i) The solute restricts the *orientational freedom* of each pair of neighboring waters in the first shell through new geometric constraints that can be treated fully within the same integrations as in the Cage water liquid model. (ii) The solute molecule interacts with each water through a term ϵ_{SW} in eq 7, which contains both enthalpic and entropic components. These two effects are shown in Figure 2.

i. Solute Insertion Imposes Geometrical Orientational Restrictions on First-Shell Water Hydrogen Bonding. Inserting a solute into water affects the first-shell waters in multiple ways. First, Figure 2 shows how the insertion of a spherical solute into bulk water causes a restriction of first-shell water−water hydrogen-bonding angles.

In the calculation of the orientational entropy and average energy of the first hydration shell waters, an analytical geometric approach was used to determine the number of H-bonds one water can make with the other water as a function of rotation angle of one water over the other. The larger the radius of the solute is, the more it restricts first-shell water−water hydrogen-bonding angles.[26] This geometric restriction can be determined through a fast analytical calculation (see Supporting Information). This geometric restriction reduces the orientational entropy of the first shell water, and it also changes the average energy of the first shell water.

ii. Solute Insertion Entails Interaction Energetics with First-Shell Waters. We now develop an expression for the solute water interaction quantity, ϵ_{SW} in eq 7. Keeping consistent with the microscopic physics of the Cage Water model and from our previous study,[27] we recognize that $\epsilon_{SW} = \epsilon_{SW}(r, T)$ is not simply a constant but will depend on solute radius r and temperature T. We use the following function:

$$\epsilon_{SW}(r, T) = (a_1 + a_2 r^2) + (b_1 + b_2 r^2)T - (f_1 + f_2 r + f_3 r^2)T \ln T \quad (9)$$

Here the coefficients a, b, and f are constant-value parameters of the model. Their values are given in Table S1 (for full details of the parameters, see the Supporting Information). Note that eq 9 is in reduced units; the version with physical units is given by eq S23 in the Supporting Information. The values of the parameters, in physical units, are given in Table 1.

Table 1. Values of the Parameters Used in the Solute−Water Interaction Term[a]

parameters	set 1	set 2
$a_1\left(\frac{\text{kJ}}{\text{mol}}\right)$	0.29	−3.05
$a_2\left(\frac{\text{kJ}}{\text{mol Å}^2}\right)$	−1.03	−0.14
$b_1\left(\frac{\text{kJ}}{\text{mol K}}\right)$	33.98	41.10
$b_2\left(\frac{\text{kJ}}{\text{mol K Å}^2}\right)$	3.77	2.61
$f_1\left(\frac{\text{kJ}}{\text{mol K}}\right)$	16.57	3.60
$f_2\left(\frac{\text{kJ}}{\text{mol K Å}}\right)$	−32.46	−14.19
$f_3\left(\frac{\text{kJ}}{\text{mol K Å}^2}\right)$	7.01	0.64

[a]Set 1 is for inert gases. Set 2 is for molecular solutes (CH_4, C_6H_6, $C_{10}H_8$, C_{60}).

Here is the basis for these terms. First, for fixed r, the temperature dependence of water's interaction with a solute surface will have approximately a constant heat capacity; thus, the lowest-order expansion for the interaction free energy will be given by $d_0 + d_1 T + d_2 T \ln T$, where the d's are constant coefficients. This constant heat capacity is among the simplest

https://doi.org/10.1021/acs.jpcb.2c02695
J. Phys. Chem. B XXXX, XXX, XXX−XXX

Table 2. Values of the Solute Radii

solute	He	Ne	Ar	Kr	Xe	Rn	CH_4	C_6H_6	$C_{10}H_8$	C_{60}
radius (Å)	1.43	1.58	1.94	2.07	2.28	2.4	2.06	3.36	4.46	5.01

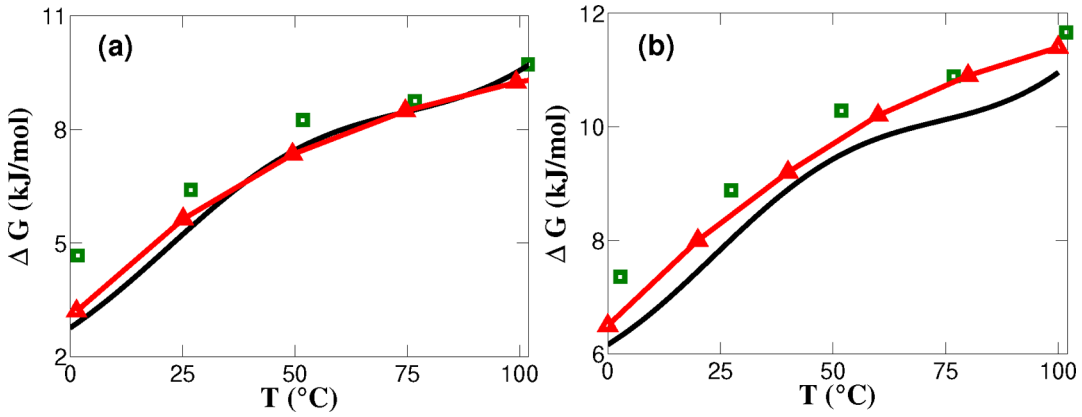

Figure 3. Comparing solvation free energies, from the Crustwater theory (black line), TIP4P/2005 simulations (green squares),[20] and experiments (red triangles, with line fit). (a) Xe and (b) CH_4.

forms and is known from experiments of vicinal water molecules at surfaces.[28] The physical explanation for why this surface interaction should have any heat capacity at all is that temperature affects first-shell waters differently than the bulk by reducing their hydrogen bonding. It results in increasing their relative LJ bonding, and increasing the translational entropy by loosening contacts of the solute with the first shell. Second, for a fixed temperature, each of the d terms is a polynomial in solute radius r, accounting for the cost of creating a cavity in water, according to scaled-particle theory.[57]

Our procedure for calculations is as follows. (a) First, we compute the solute−water effective free energy ϵ_{SW} using the parameters in Table 1. (b) Then the average energy of one water−both with the solute ($\langle\epsilon(\zeta(\theta_0))\rangle_h$) and without the solute ($\langle\epsilon\rangle_b$) is calculated using eqs 7 and 8, respectively. (c) Then, the partition functions of an average water in the presence of solute (q_h) and absence of solute (q_b) are calculated using eqs 5 and 6, respectively. (d) We then substitute these values into eq 4 to get the solvation free energy. Standard thermodynamic relations then give the enthalpy, entropy and specific heat capacity as a function of temperature, pressure and solute size.

Table 1 gives the parameters we used in eq S23 after converting ϵ_{SW} to physical units. The conversion procedure is explained in the Supporting Information. Table 2 gives the solute radii we used: the radii for inert gases are taken from Vogt et al.;[29] for methane, from Kammeyer et al.;[30] for benzene from Steinruck et al.;[31] and for C_{60} from Muthukrishnan et al.[32]

RESULTS AND DISCUSSION

In the next few paragraphs, first we compare our results to MD simulations of TIP4P/2005 water model with two different treatments for the solute model, then we give results of the model calculations for six inert gases of the nonpolar solvation thermodynamics—the free energy, enthalpy, entropy, and heat capacity—as functions of temperature and pressure, over the full range of liquid water. We compare the temperature dependences against available experimental data.

Comparing the Crustwater Model to TIP4P/2005 MD Simulations. The present model predicts the free energy, $\Delta G(T)$ of solute transfer of small nonpolar solutes into water about as accurately as the best explicit-water MD simulations. Guillot et al., in a pioneering work, calculated hydration thermodynamics using Widom's particle insertion method for four inert gases and methane.[4] They stated that their inaccuracies in reproducing experimental solubilities was attributable to short simulations, in some cases uncertainty in the experiments, and accuracy of potential energy functions, even with the addition of a polarization term. Pascheck took the same five solutes with five different explicit water models also using Widom's insertion method.[5] He found that at low temperatures (around 275 K) all water models except TIP5P overestimate the free energies for both xenon and methane. Dyer et al.[20] achieved better agreement by using a polarizable model for the solutes and the TIP4P (nonpolarizable) explicit water model, using recent parametrizations TIP4P/2005 and TIP4P/EW. Figure 3 compares our Crustwater calculations with Dyer's TIP4P/2005 simulations and with experimental data for solutes Xe and CH_4 for hydration free energy. The Crustwater model is quite good over the full liquid water range.

Also, in Figure 4, we compared our results to another TIP4P/2005 MD simulations in the liquid water range for Ar.[33] In this simulational study, solutes were modeled using LJ potentials optimized to reproduce the experimentally known hydration free energy at 25°C and 1 bar.[34] We found that our predictions for the hydration free energy are very close to their results for Ar taken as an LJ particle but with a slightly different curvature, which results in some deviation for the hydration enthalpy and hydration entropy.

Solvation of Nonpolar Inert Gases: Temperature Dependences. Figure 5 compares experimental and calculated hydration free energy (ΔG), enthalpy (ΔH), entropy (ΔS), and specific heat at constant pressure (ΔC_p), against temperature, for three noble gases, Ar, Kr, and Xe. Only three are presented here to avoid crowding the figure; the results for He, Ne, and Rn are shown in Figure S8. The agreement with experiments is good, although the downward curvature for Rn is not correctly captured.

https://doi.org/10.1021/acs.jpcb.2c02695
J. Phys. Chem. B XXXX, XXX, XXX−XXX

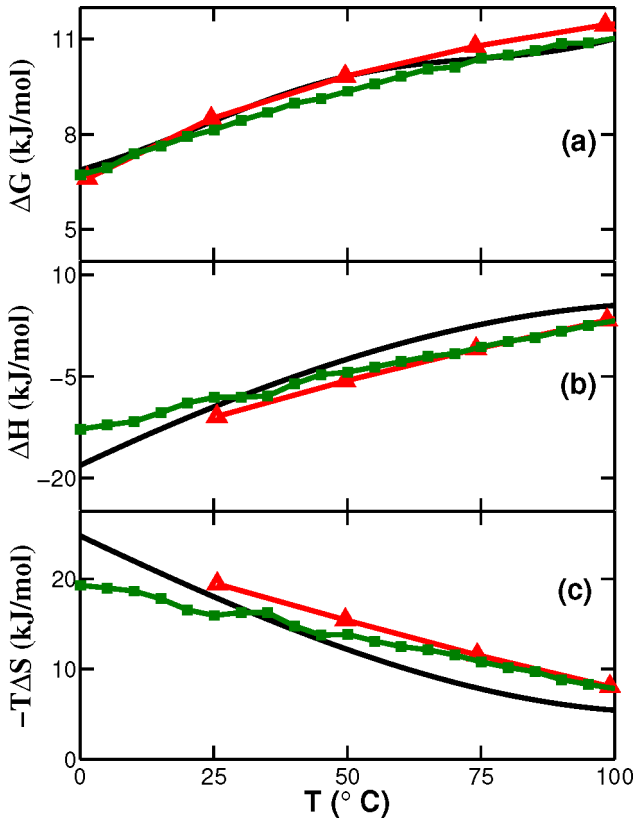

Figure 4. Temperature dependence of thermodynamic quantities for Ar, comparing our Crustwater theory (black lines) with experiments (red triangles, with line fit) and Ashbaugh et al. MD data (green squares, with line fit).[33]

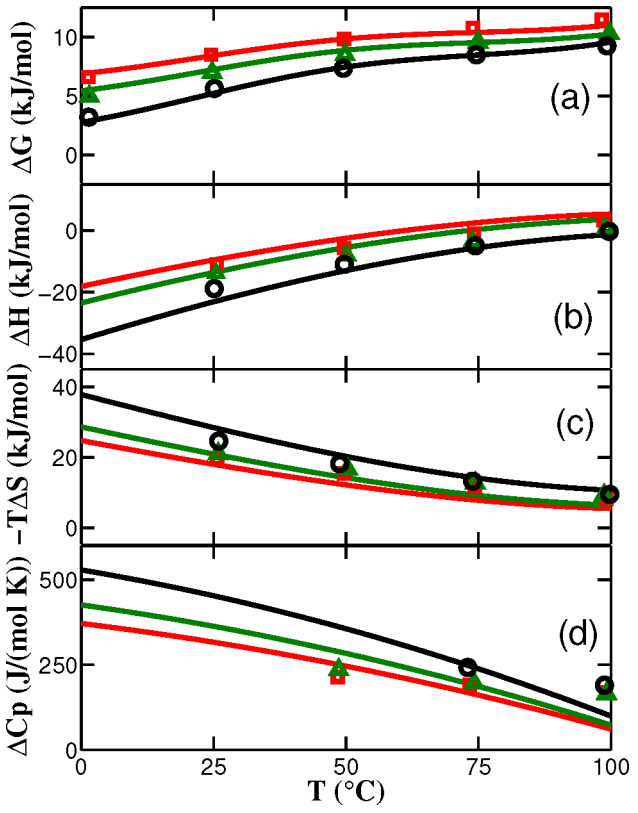

Figure 5. Temperature dependences of thermodynamic properties of inert gases. Comparison between experimental values (symbols)[35−37] and theory (line). Color code: red (Ar), green (Kr), and black (Xe). Results for other inert gases are shown in the Supporting Information (Figure S8).

Larger Molecular Solutes: Temperature Dependence. Beyond the inert gases, we also looked at small nearly spherical molecules—methane (Figure 6a−d) and benzene (Figure 6e−h). For these molecules too, predictions agree well with experiments, including qualitatively the heat capacities. The parameters we used for the molecular solutes−methane, benzene, naphthalene, and fullerene—are given in Table 1. For naphthalene, and fullerene, experimental data is only available for room temperature; results are in Figure 10.

The Basic Interpretation of Solvation Thermodynamics. The longstanding rule that *oil and water do not mix* and its unusual temperature dependence, which has motivated the term *the hydrophobic effect*, have a well-known interpretation in the experimental data above. Dissolving these solutes in cold water (around 0−25 °C) is unfavorable; i.e., $\Delta G > 0$. (The exception is benzene, which has a slightly favorable ΔG of insertion in cold water. We return to benzene below.) Second, in cold water, the solvation enthalpy, ΔH, is negative (favorable) and the corresponding entropy contribution, $-T\Delta S$, is positive (unfavorable). This is the basis for the view that inserting solutes into cold water is opposed by the water structuring it induces. Now consider hot water. In hot water, much of the water's structure is melted out, so (a) the entropy cost of inserting a solute is less than in cold water and (b) the solute−water interactions are less attractive. Inserting a small nonpolar solute into hot water only induces weak favorable and unfavorable components. This temperature dependence is captured well by recognizing that solvation entails a heat capacity of transfer. And, for these simple solutes, this heat capacity of transfer is not strongly dependent on temperature. The Crustwater predictions are mostly consistent with these basic interpretations.

Benzene is slightly different. Solvating benzene in cold water is slightly favorable. Our calculations are for the free energy change in dissolving benzene from the gas phase in liquid water. If, instead, benzene is transferred from liquid benzene to water, it would be necessary to also include the free energy of evaporation of liquid benzene to its gas phase. Benzene's additional favorable enthalpy in water may come from its partial charge or multipole or polarizable interactions with water.[42−44]

Analyzing the Model's Microscopic Basis for Solvation's Structure−Property Relations. Returning to the simpler solutes, the Crustwater model gives additional insights. As others have done before,[45−47] we decompose the hydration free energy (given by eqs 2−4) into

$$\Delta G = \Delta G_{SW} + \Delta G_{WW} \tag{10}$$

where SW and WW are the solute−water and water−water components, respectively. Also, we note that $\Delta G_{SW} = 0.5n(r)\epsilon_{SW}$ with $n(r)$ as the average number of water molecules in the first solvation shell of the solute, from the eq 12 given later. We further decompose this into enthalpy H and entropy S components as

$$\Delta G = \Delta H_{SW} + \Delta H_{WW} - T[\Delta S_{WW} + \Delta S_{SW}] \tag{11}$$

where T is temperature. In short, here is the model conception of solvation. At a given temperature or pressure, the water molecules in the bulk or in the surface crust (first solvation

https://doi.org/10.1021/acs.jpcb.2c02695
J. Phys. Chem. B XXXX, XXX, XXX−XXX

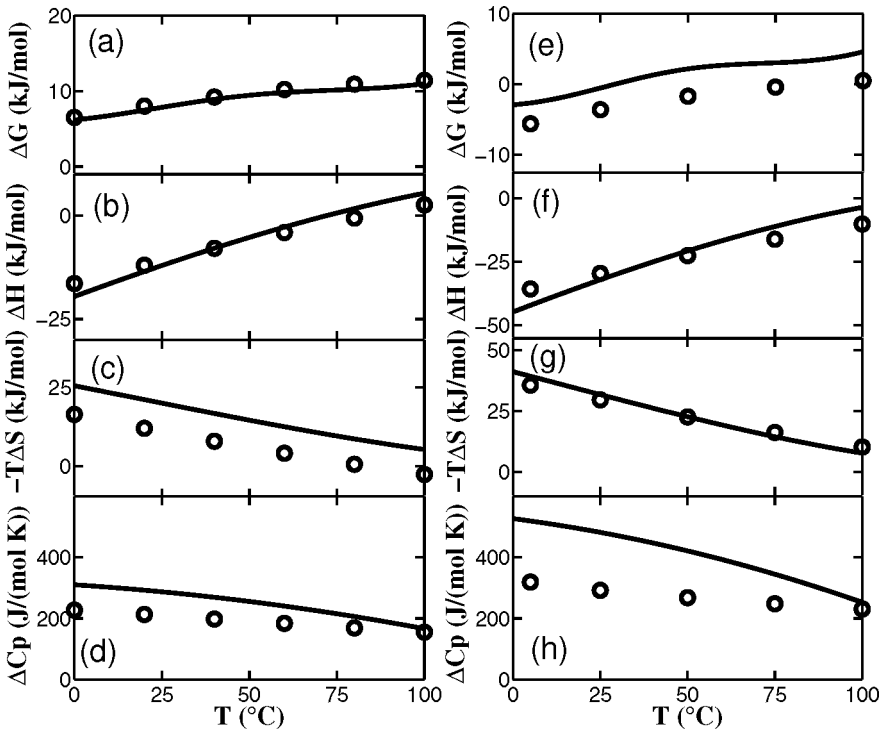

Figure 6. Temperature dependence of methane (a–d) and benzene (e–h), theory (line) vs experiments (symbols).[38−41]

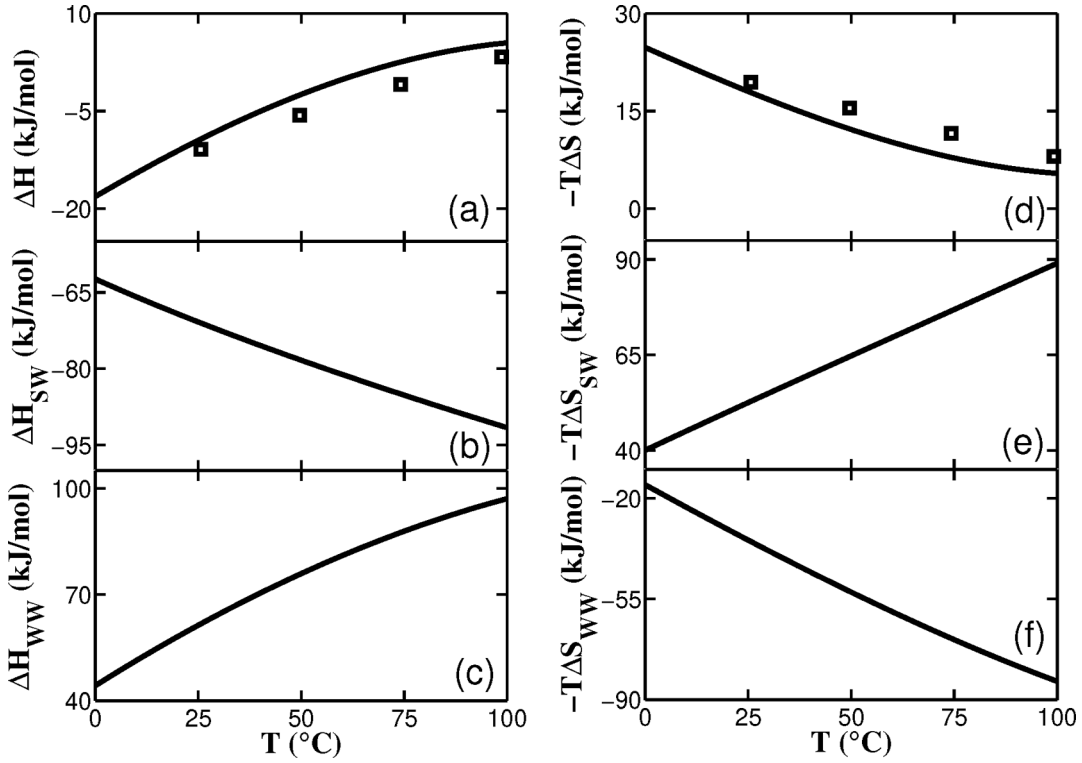

Figure 7. WW and SW components of the enthalpy and entropy components of solvation free energy vs temperature, for Ar. Symbols are experimental data. The top line just shows the totals given in Figure 5.

shell) are distributed according to the Cage Water model of pure water for those conditions. Some water pairs are H-bonded, some are LJ bonded, and some are noninteracting. Step one of solvation (labeled as WW) is the insertion of a *steric ghost* solute having the correct radius, but with the solute−water interaction turned off, $\epsilon_{SW} = 0$. Only those cavities having the appropriate water−water H-bond orientations in the crust are picked out at this step. Step two of solvation (labeled as SW) entails turning on the SW interaction, within the appropriate cavity.

Figure 7 shows the contributions of the WW and SW terms to the solvation enthalpy and entropy in the model. For cold

https://doi.org/10.1021/acs.jpcb.2c02695
J. Phys. Chem. B XXXX, XXX, XXX−XXX

water (left side of the figures), the solvation enthalpy, which is negative (i.e., favorable), is dominated by the SW term. This represents the energetic attraction that results from turning on the interaction of the solute with the crust water molecules in the first solvation shell. There is also a WW solvation enthalpy component, which entails breaking water−water interactions. And, while the WW term is unfavorable and opposes the SW component, it is smaller than the SW term. For the hot water, each water has more entropy as compared to cold water; therefore, to make a crust around the solute the SW enthalpy becomes more favorable while the WW is more unfavorable due to excessive breaking of HBs at a higher temperature.

Next, consider the solvation entropy component in cold water. Inserting solute into water is opposed by the total entropy, $-T\Delta S$. This entropy is dominated by the SW interaction, not the WW orientational restrictions in the crust, which are given by the WW term. (In more detail, the WW entropy change has two parts: (a) the steric ghost solute restriction entropy, which is unfavorable and (b) the entropy of breaking of hbonds between waters, which is favorable.) Therefore, we interpret the oil-in-water unfavorability in cold water as being dominated by the free-volume (translational) change. These interpretations are supported by the more granular breakdown of components of ϵ_{SW} shown in parts b and e of Figure 7. When solute inserts into cold water, the crust contracts around it and this tightening is reflected in the translational entropy shown in Figure 7e.

Now, consider the solvation entropy in hot water. While the net solvation entropy, $-T\Delta S$, is small for solutes in hot water, it is composed of large opposing SW and WW terms. Whereas in cold water, the crust is relatively confined around the solute, in hot water, there is an additional translational entropy cost in recruiting water molecules from the surroundings to form a solvation crust. This conclusion is robust to different choices of model parameters. Figure 8b shows that $-T\Delta S_{WW}$ is dominated by the loss of hydrogen bonding. And, $-T\Delta S_{WW}$ cannot be positive as the maximum value of this term will be zero when there is no H-bond loss. So, $-T\Delta S_{SW}$ will always dominate.

We now look to the model for additional microscopic insights into the WW interactions. For this, we express the hydration free energy in terms of the microscopic model quantities as

$$\Delta G = n(r)[\langle u_{HB}\rangle f_{HB}\{0.5\zeta(\theta_0) - 2\} + \langle u_{cage}\rangle f_{cage}\{0.5\zeta(\theta_0) - 2\} + p\{v^h_{mol} - v^b_{mol}\} + 0.5\epsilon_{SW}] \quad (12)$$

where we can define the first two terms as a hydrogen-bonding orientational restriction in the crust, ΔG_{HB}; the third term as resulting from pressure−volume changes, ΔG_v; and the fourth term as the quantity we have previously labeled ΔG_{SW}. Also, recall that $\Delta G_{WW} = \Delta G - \Delta G_{SW}$. Of course, eq 12 can also be parsed into enthalpy and entropy components, $\Delta G = \Delta H - T\Delta S$. These quantities are shown in Figure 8. For reference, panel c of Figure 8 shows the fractional populations of different states of pure Cage Water. Panels a and b of Figure 8 confirm that the WW steric ghost contributions to free energy are given almost exclusively by the water−water hydrogen-bonding term in the crust. Both the water−water enthalpy and entropy increase monotonically with temperature, in parallel with the loss of H-bonds in the bulk (panel c).

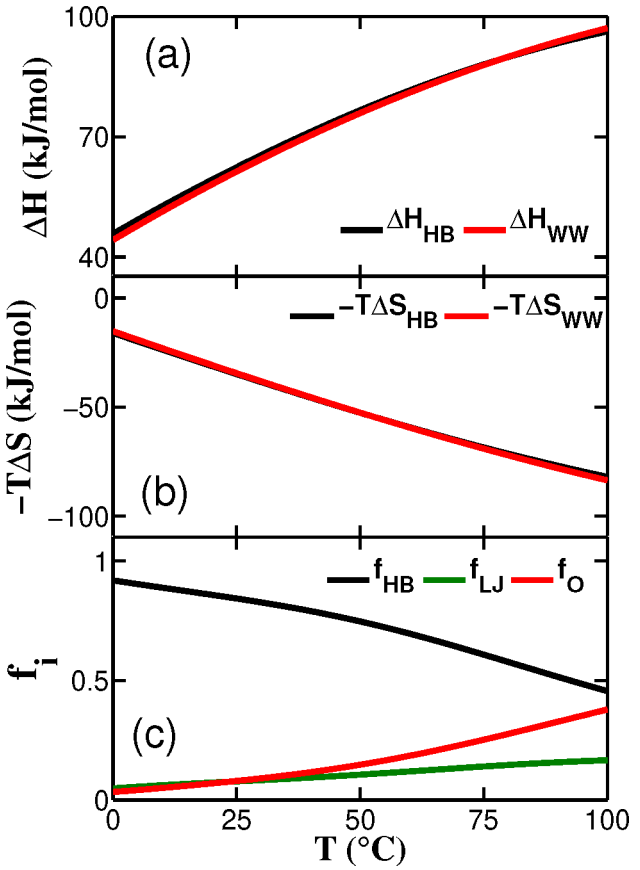

Figure 8. Contribution of average hydrogen bond energy to the water−water components of (a) the solvation enthalpy, (b) $-T\Delta S$ vs temperature for Ar, and (c) the fractional populations of the states. Here, HB represents both pairwise as well as co-operative HB states.

Pressure Dependence of Solvation. Figure 9 shows the predicted pressure dependences of the thermodynamic quantities at 298 K for Ar and methane. Results for other inert gases, He, Ne, Kr, Xe, and Rn are shown in the Supporting Information Figure S9. On the x-axis, the reduced pressure that we used in the calculation has been scaled to pressure in units of atmospheres using the equivalence of the population of the cage state between the current model and the Cage Water reference model.[21] The ΔG values are scaled by using the value obtained in Figure 5 for the given thermodynamic states of T, p. The positive slope of ΔG with pressure is consistent with previous experiments[48] and theory.[6] Experimental measurements by Kennan et al.[48] show that ΔG increases with pressure for Ar, Kr, and Xe, but the rate of increase was smaller than that given by our model.

Figure 9 (black lines) shows predicted pressure effects on methane solvation. We are unaware of any experimental data, but we compare in the Supporting Information (Figure S12) with simulation results from Chan.[6] The fact that ΔG increases with pressure in our calculations is consistent with the MD modeling of Koga et al.[49] We have also compared our results with a recent MD simulation data[34] for the pressure dependence in the common range of the pressure between both studies, i.e., 0 to 1000 atm in the Supporting Information Figure S11. For smaller inert gas solutes (He and Ne), we see that our model is in good quantitative agreement to their results. However, for other inert gases and methane, we get only the qualitative agreement.

https://doi.org/10.1021/acs.jpcb.2c02695
J. Phys. Chem. B XXXX, XXX, XXX−XXX

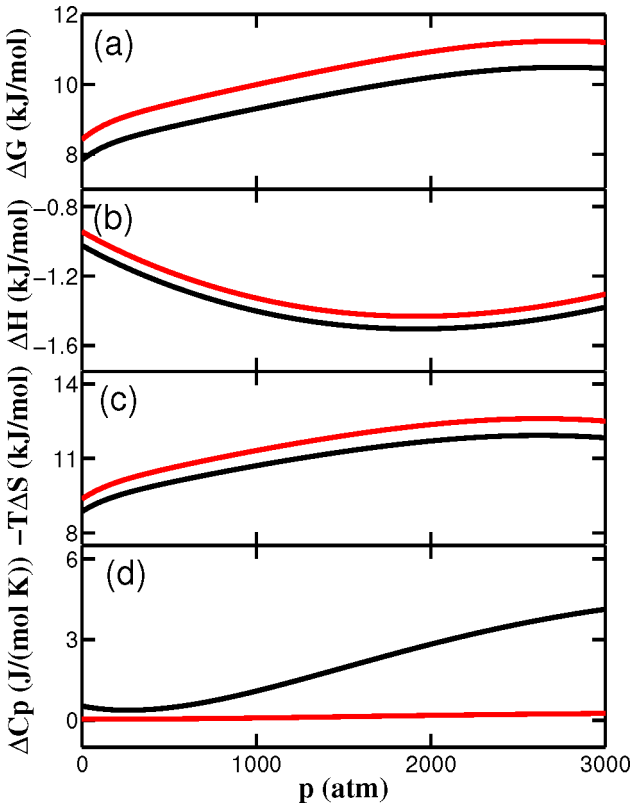

Figure 9. Predicted pressure dependences of solvation thermodynamic quantities: argon (red) and methane (black).

To summarize this section, we can conclude that our model gives only qualitative and in some cases, semiquantitative, match with the previous simulations results. This is because, in our model, we do not have any pressure dependent parameters or features that can be introduced to have a better match with previous work for pressure dependence solvation thermodynamics.

Solvation Thermodynamics Dependence on Solute Radius. Figure 7 and eq 12 show that the water−water terms ΔH_{WW} and ΔS_{WW} depend only on the solute radius and not on its chemical nature. The chemical nature of the solute only enters through the SW terms. For solutes that are big enough, growing the solute size will proportionately "push out" the WW crust, growing the crust surface area in proportion to the solute area. It follows that the free energy of transfer divided by the solute area should be a constant for a given series of solutes of increasing radii. However, if solutes are small enough to rattle around inside a water cage, then growing their small size further should not push out the crust (until they reach the size that does). Years ago, simple models predicted there would be a crossover in thermal behavior of $\Delta G/(\text{area})$ from very small solute radii to larger solutes, reaching a constant plateau for sufficiently large solutes.[50,51] The Lum−Chandler−Weeks model, based on cavity fluctuations, predicted a nanoscale crossover size, of around 10−20 Å for hard sphere (HS) solutes. In contrast, the Southall−Dill model, based on the average crust size arguments above, predicted a smaller crossover radius, of 1−2 Å.

Now, we can say more, both because there is now extensive experimental data and because the Crustwater model gives

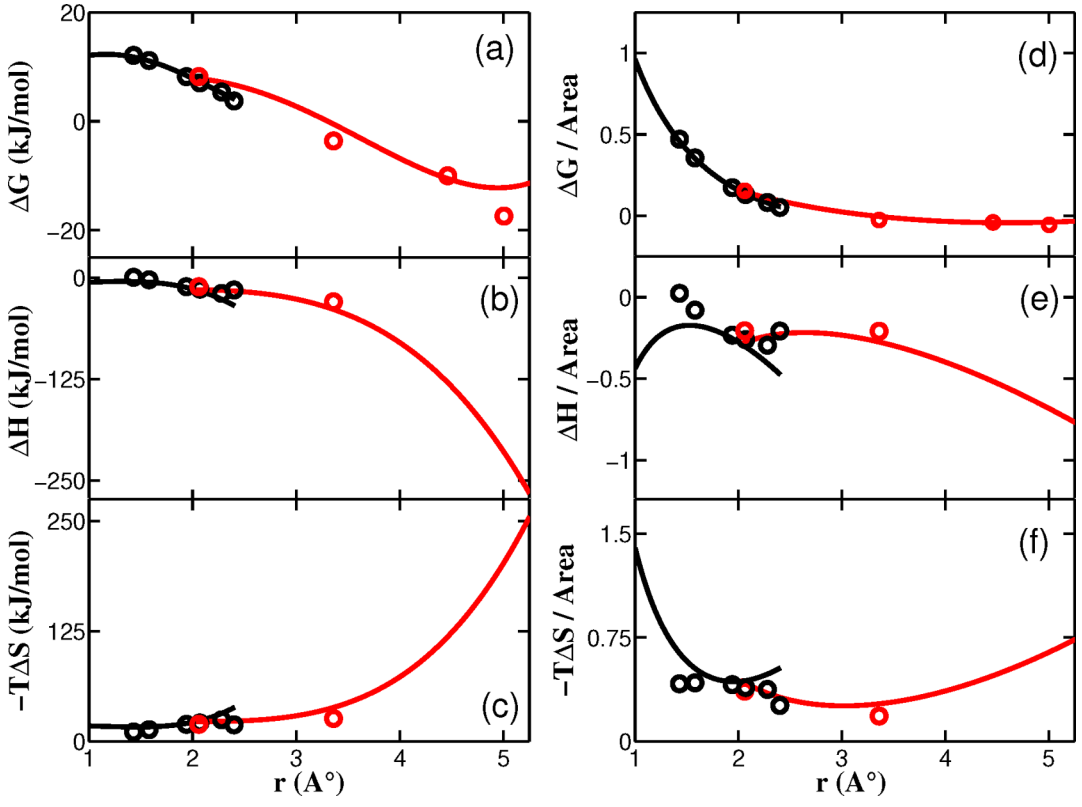

Figure 10. (a−c) Size dependences of solvation thermodynamics between theory (lines) and experiment (symbols) for inert gases and hydrocarbons. (d−f) The same quantities divided by area with unit kJ/(mol Å^2) at T = 298.15 K and p = 1 atm. The color code is black = He, Ne, Ar, Kr, Xe, and Rn and red = CH_4, C_6H_6, $C_{10}H_8$, and C_{60} in the sequence of their increasing size.

https://doi.org/10.1021/acs.jpcb.2c02695
J. Phys. Chem. B XXXX, XXX, XXX−XXX

additional tests. Figure 10d shows that the Crustwater model bears out these earlier qualitative expectations of a crossover to a plateau. In addition, the model gives quantitative agreement with experiments on both inert gases and small hydrocarbons. First, it shows that the crossover radius is around 2 Å. Second, it shows also the enthalpy and entropy components of these size effects in panels b and c and panels e and f of Figure 10. As solutes shrink to very small sizes, the solute−water interactions weaken because they are looser and the entropy of caging is unaffected.

However, there are two points to be considered to see our results vis-à-vis LCW results: (1) our model is not treating a large oil−water interface, but rather it is treating the surface area dependence of the free energy of hydration of quasi-spherical solutes in water; (2) our model has realistic solute−water attractive interaction producing results close to the experimental one. Hence, the results in Figure 10 are coming from both surface area dependence and the chemical nature of the solutes (in contrast to the HS results from LCW[50]).

Caveats and Comments on the Model. Water is complex in ways that have required different models, different trade-offs and different levels of rigor for different properties. In developing the present model, we have favored the following: (i) physicality, but with simplicity and interpretability, (ii) speed in computations, and (iii) accuracy in capturing experimental data. In this and the Cage Water model of the pure liquid on which it rests, we start from three interaction types (hydrogen bonding, Lennard-Jones, and cooperative cage H-bonding) and express a partition function in which configurational enumerations are done based on a tetrahedral-lattice-like underlying symmetry. Introducing a spherical nonpolar solute induces geometric restrictions in first-shell waters that are treated in the same way. For the microphysics of the energetics of the solute−water interaction, we use a form motivated by scaled-particle theory. This modeling strategy of separation into two terms—a statmech counting term and a parametrized microphysics term—is in a longstanding spirit of modeling in colloids, polymers, liquids, and biomolecules. The Flory−Huggins theory of polymer solutions, for example, has a lattice chain counting procedure and a Flory χ parameter that itself typically contains parametrized complexity of monomer−solvent details;[52] similarly in the Wertheim theory of associating fluids and other complex fluids.[53] Later, improvements may be possible. But, the present work offers excellent speed. Our calculations take less than a second for the whole free energy curve with our Python code. Moreover, our model has no statistical error which often makes the rationalization of the results difficult with computer simulation methodology. It gives a wide range of fairly accurate predictions over temperature and solute radius that are not otherwise available. And, the model gives interpretations of the observables on the basis of water structure and energies and solute size. Our work can be compared with a recent information theory-based model developed by Ashbaugh, Vats, and Garde,[54] which shows that the temperature dependence of hydrophobic hydration for hard-sphere solutes with varying sizes such as water's density and compressibility, can be captured with only a few parameters. And Patel[55] also includes a solute−water attractive interaction in an information-theory-based model. Such models assume (1) that the relevant fluctuations come from water's density and (2) that, for small fluctuations, the distribution is Gaussian. In the present model instead, we consider both density and water orientations to be critical for water properties, and we do not assume a Gaussian distribution of fluctuation. Our starting point instead is a physical partition function. The physical basis of our model is similar to a pioneering work by Rossky and Zichi, who found that the distribution of local energies in the solvation shell around a hydrophobic solute gets sharper as compared to that in the absence of a solute.[56] This in turn suggests that water−water interactions in the hydration shell are tighter than that in the bulk water. Our model agrees with this. In our case, the microscopic basis for it is in the geometry of water−water orientations. In our model, the hydrophobic solute reduces the orientational freedom of one water relative to its neighbor.

CONCLUSIONS

We have developed an analytical model of solvation thermodynamics for (quasi) spherical gases, both atomic and molecular. The results are in mostly excellent agreement with experiments. This almost instantaneous calculation comes from treating the solvation in terms of a cage water model. The geometrical changes and, in particular, the change of average number of H-bonds each water can make with other waters have been calculated with an innovative geometrical approach. The energy of interaction between solute and water has been represented by an effective free energy. The model gives some insights into the structural basis for the hydrophobic effect. First, it shows that, in cold water, the enthalpy and entropy are dominated by SW interactions, while in hot water, they are dominated by WW interactions. In cold water, solutes dissolve because of SW attractions, but the oil−water insolubility is opposed by the translational entropy of tight packing. Raising the temperature leads to a breaking of WW hydrogen bonds and a more favorable WW entropy. Second, the model, combined with experimental data shows that shrinking solutes to below the size of a water cage, leads to a "rattling around", a weakening of interactions without much effect on the water cage.

ASSOCIATED CONTENT

Supporting Information

The Supporting Information is available free of charge at https://pubs.acs.org/doi/10.1021/acs.jpcb.2c02695.

Detail of the parameters and additional plots (PDF)

AUTHOR INFORMATION

Corresponding Author

Ken A. Dill − *Laufer Center for Physical and Quantitative Biology; Department of Physics and Astronomy ; Department of Chemistry, Stony Brook University, Stony Brook, New York 11794, United States;* orcid.org/0000-0002-2390-2002; Email: dill@laufercenter.org

Authors

Ajeet Kumar Yadav − *School of Computational and Integrative Sciences, Jawaharlal Nehru University, New Delhi 110067, India*

Pradipta Bandyopadhyay − *School of Computational and Integrative Sciences, Jawaharlal Nehru University, New Delhi 110067, India;* orcid.org/0000-0001-6343-623X

Evangelos A. Coutsias − *Department of Applied Mathematics and Statistics ; Laufer Center for Physical and Quantitative*

https://doi.org/10.1021/acs.jpcb.2c02695
J. Phys. Chem. B XXXX, XXX, XXX−XXX

Biology, Stony Brook University, Stony Brook, New York 11794, United States; orcid.org/0000-0003-2910-9125

Complete contact information is available at: https://pubs.acs.org/10.1021/acs.jpcb.2c02695

Notes

The authors declare no competing financial interest.

■ ACKNOWLEDGMENTS

K.A.D. and E.A.C. acknowledge funding from NIH Grant RM1 GM135136 and the Laufer Center for Physical and Quantitative Biology at Stony Brook University. A.K.Y. and P.B. acknowledge the support from the Department of Biotechnology grant (BT/PR40251/BITS/137/11/2021) awarded to the Center for Computational Biology and Bioinformatics, Jawaharlal Nehru University.

■ DEDICATION

We dedicate this paper to Pablo Debenedetti, in honor of this Festschrift on the occasion of his 70th birthday. Happy Birthday, Pablo! With great respect for his pioneering research in liquids, water, and glasses; with great warmth from K.A.D. from years of close personal friendship; and with great appreciation for truly exceptional shared then-junior colleagues, Tom Truskett and Scott Shell.

■ REFERENCES

(1) Straatsma, T. P.; Berendsen, H. J. C.; Postma, J. P. M. Free Energy of Hydrophobic Hydration: A Molecular Dynamics Study of Noble Gases in Water. *J. Chem. Phys.* **1986**, *85*, 6720−6727.

(2) Guillot, B.; Guissani, Y.; Bratos, S. A Computer-Simulation Study of Hydrophobic Hydration of Rare Gases and of Methane. I. Thermodynamic and Structural Properties. *J. Chem. Phys.* **1991**, *95*, 3643−3648.

(3) Tanaka, H.; Nakanishi, K. A Computer-Simulation Study of Hydrophobic Hydration of Rare Gases and of Methane. I. Thermodynamic and Structural Properties. *J. Chem. Phys.* **1991**, *95*, 3719−3727.

(4) Guillot, B.; Guissani, Y. A. A Computer-Simulation Study of Hydrophobic Hydration of Rare Gases and of Methane. I. Thermodynamic and Structural Properties. *J. Chem. Phys.* **1993**, *99*, 8075−8094.

(5) Paschek, D. Temperature Dependence of the Hydrophobic Hydration and Interaction of Simple Solutes: An Examination of Five Popular Water Models. *J. Chem. Phys.* **2004**, *120*, 6674−6690.

(6) Moghaddam, M. S.; Chan, H. S. Pressure and Temperature Dependence of Hydrophobic Hydration: Volumetric, Compressibility, and Thermodynamic Signatures. *J. Chem. Phys.* **2007**, *126*, 114507.

(7) Dowdle, J. R.; Buldyrev, S. V.; Stanley, H. E.; Debenedetti, P. G.; Rossky, P. J. Pressure and Temperature Dependence of Hydrophobic Hydration: Volumetric, Compressibility, and Thermodynamic Signatures. *J. Chem. Phys.* **2013**, *138*, 064506.

(8) Cerdeiriña, C. A.; Debenedetti, P. G. Debenedetti Water Anomalous Thermodynamics, Attraction, Repulsion, and Hydrophobic Hydration. *J. Chem. Phys.* **2016**, *144*, 164501.

(9) Frank, H. S.; Evans, M. W. Free Volume and Entropy in Condensed Systems III. Entropy in Binary Liquid Mixtures; Partial Molal Entropy in Dilute Solutions; Structure and Thermodynamics in Aqueous Electrolytes. *J. Chem. Phys.* **1945**, *13*, 507−532.

(10) Southall, N. T.; Dill, K. A.; Haymet, A. D. J. A. View of the Hydrophobic Effect. *J. Phys. Chem. B* **2002**, *106*, 521−533.

(11) Brini, E.; Fennell, C. J.; Fernandez-Serra, M.; Hribar-Lee, B.; Lukšič, M.; Dill, K. A. How Water's Properties Are Encoded in Its Molecular Structure and Energies. *Chem. Rev.* **2017**, *117*, 12385−12414.

(12) Levy, Y.; Onuchic, J. N. Water Mediation in Protein Folding and Molecular Recognition. *Annu. Rev. Biophys. Biomol. Struct.* **2006**, *35*, 389−415.

(13) Einserberg, D.; W, K. *The Structure and Properties of Water*; Oxford University Press: New York, 2005.

(14) Chan, H. S. Modeling Protein Density of States: Additive Hydrophobic Effects Are Insufficient for Calorimetric Two-State Cooperativity. *Proteins Struct. Funct. Genet.* **2000**, *40*, 543.

(15) Dill, K. A. Dominant Forces in Protein Folding. *Biochemistry* **1990**, *29*, 7133−7155.

(16) Kuffel, A.; Zielkiewicz, J. Why the Solvation Water around Proteins Is More Dense than Bulk Water. *J. Phys. Chem. B* **2012**, *116*, 12113−12124.

(17) Eisenberg, D.; McLachlan, A. D. McLachlan Solvation Energy in Protein Folding and Binding. *Nature* **1986**, *319*, 199−203.

(18) Baldwin, R. L. Temperature dependence of the hydrophobic interaction in protein folding. *Proc. Natl. Acad. Sci. U. S. A.* **1986**, *83*, 8069−8072.

(19) Xie, G.; Timasheff, S. N. Preferential Interactions of Urea with Lysozyme and Their Linkage to Protein Denaturation. *Biophys. Chem.* **2003**, *105*, 421−448.

(20) Dyer, P. J.; Docherty, H.; Cummings, P. T. The importance of polarizability in the modeling of solubility: Quantifying the effect of solute polarizability on the solubility of small nonpolar solutes in popular models of water. *J. Chem. Phys.* **2008**, *129*, 024508.

(21) Urbic, T.; Dill, K. A. Water Is a Cagey Liquid. *J. Am. Chem. Soc.* **2018**, *140*, 17106−17113.

(22) Abascal, J. L.; Vega, C. A general purpose model for the condensed phases of water: TIP4P/2005. *J. Chem. Phys.* **2005**, *123*, 234505.

(23) Urbic, T. Liquid-Liquid Critical Point in a Simple Analytical Model of Water. *Phys. Rev. E* **2016**, *94*, 1−5.

(24) Urbic, T. Analytical Model for Three-Dimensional Mercedes-Benz Water Molecules. *Phys. Rev. E* **2012**, *85*, 061503.

(25) Urbic, T.; Dill, K. A. Analytical Theory of the Hydrophobic Effect of Solutes in Water. *Phys. Rev. E* **2017**, *96*, 1−12.

(26) Kim, J.; Tian, Y.; Wu, J. Thermodynamic and structural evidence for reduced hydrogen bonding among water molecules near small hydrophobic solutes. *J. Phys. Chem. B* **2015**, *119*, 12108−12116.

(27) Yadav, A. K.; Bandyopadhyay, P.; Urbic, T.; Dill, K. A. Analytical 2-Dimensional Model of Nonpolar and Ionic Solvation in Water. *J. Phys. Chem. B* **2021**, *125*, 1861−1873.

(28) Etzler, F. M.; Conners, J. J. Temperature Dependence of the Heat Capacity of Water in Small Pores. *Langmuir* **1990**, *6*, 1250−1253.

(29) Vogt, J.; Alvarez, S. Van Der Waals Radii of Noble Gases. *Inorg. Chem.* **2014**, *53*, 9260−9266.

(30) Kammeyer, C. W.; Whitman, D. R. Quantum Mechanical Calculation of Molecular Radii. I. Hydrides of Elements of Periodic Groups IV through VII. *J. Chem. Phys.* **1972**, *56*, 4419−4421.

(31) Steinrück, H.-P.; Huber, W.; Pache, T.; Menzel, D. THE ADSORPTION ON Ni(Ll1) SCUD H.-P. STEINRUCK. *Surf. Sci.* **1989**, *218*, 293−316.

(32) Muthukrishnan, A.; Sangaranarayanan, M. V. Hydration Energies of C60 and C70 Fullerenes - A Novel Monte Carlo Simulation Study. *Chem. Phys.* **2007**, *331*, 200−206.

(33) Ashbaugh, H. S. Reversal of the Temperature Dependence of Hydrophobic Hydration in Supercooled Water. *journal of physical chemistry letters* **2021**, *12*, 8370−8375.

(34) Ashbaugh, H. S.; Bukannan, H. Temperature, pressure, and concentration derivatives of nonpolar gas hydration: impact on the heat capacity, temperature of maximum density, and speed of sound of aqueous mixtures. *J. Phys. Chem. B* **2020**, *124*, 6924−6942.

(35) Crovetto, R.; Fernández-Prini, R.; Japas, M. L. Solubilities of Inert Gases and Methane in H_2O and in D_2O in the Temperature Range of 300 to 600 K. *J. Chem. Phys.* **1982**, *76*, 1077−1086.

(36) Krause, D.; Benson, B. B. The Solubility and Isotopic Fractionation of Gases in Dilute Aqueous Solution. IIa. Solubilities of the Noble Gases. *J. Solution Chem.* **1989**, *18*, 823−873.

(37) Lewis, C.; Hopke, P. K.; Stukel, J. J. Solubility of Radon in Selected Perfluorocarbon Compounds and Water. *Ind. Eng. Chem. Res.* **1987**, *26*, 356−359.
(38) Ben-Naim, A.; Yaacobi, M. Effects of Solutes on the Strength of Hydrophobic Interaction and Its Temperature Dependence. *J. Phys. Chem.* **1974**, *78*, 170−175.
(39) Naghibi, H.; Dec, S. F.; Gill, S. J. Heats of Solution of Methane in Water from 0 to 50°C. *J. Phys. Chem.* **1987**, *91*, 245−248.
(40) Makhatadze, G. I.; Privalov, P. L. Partial Specific Heat Capacity of Benzene and of Toluene in Aqueous Solution Determined Calorimetrically for a Broad Temperature Range. *J. Chem. Thermodyn.* **1988**, *20*, 405−412.
(41) Makhatadze, G. I.; Privalov, P. L. Energetics of Interactions of Aromatic Hydrocarbons with Water. *Biophys. Chem.* **1994**, *50*, 285−291.
(42) Graziano, G.; Lee, B. Hydration of Aromatic Hydrocarbons. *J. Phys. Chem. B* **2001**, *105*, 10367−10372.
(43) Jorgensen, W. L.; Madura, J. D.; Swenson, C. J. Optimized Intermolecular Potential Functions for Liquid Hydrocarbons. *J. Am. Chem. Soc.* **1984**, *106*, 6638−6646.
(44) Schravendijk, P.; van der Vegt, N. F. A. From Hydrophobic to Hydrophilic Solvation: An Application to Hydration of Benzene. *J. Chem. Theory Comput.* **2005**, *1*, 643−652.
(45) Muller, N. Is there a region of highly structured water around a nonpolar solute molecule? *J. Solution Chem.* **1988**, *17*, 661−672.
(46) Muller, N. Search for a realistic view of hydrophobic effects. *Acc. Chem. Res.* **1990**, *23*, 23−28.
(47) Lee, B.; Graziano, G. A Two-State Model of Hydrophobic Hydration That Produces Compensating Enthalpy and Entropy Changes. *J. Am. Chem. Soc.* **1996**, *118*, 5163−5168.
(48) Kennan, R. P.; Pollack, G. L. Pressure Dependence of the Solubility of Nitrogen, Argon, Krypton, and Xenon in Water. *J. Chem. Phys.* **1990**, *93*, 2724−2735.
(49) Koga, K.; Yamamoto, N. Hydrophobicity Varying with Temperature, Pressure, and Salt Concentration. *J. Phys. Chem. B* **2018**, *122*, 3655−3665.
(50) Lum, K.; Chandler, D.; Weeks, J. D. Hydrophobicity at Small and Large Length Scales. *J. Phys. Chem. B* **1999**, *103*, 4570−4577.
(51) Southall, N. T.; Dill, K. A. The Mechanism of Hydrophobic Solvation Depends on Solute Radius. *J. Phys. Chem. B* **2000**, *104*, 1326−1331.
(52) De Pablo, J. J.; Schieber, J. D. *Molecular engineering thermodynamics*; Cambridge University Press: 2014.
(53) Larson, R. G. *The structure and rheology of complex fluids*; Oxford university press: New York, 1999; Vol. *150*.
(54) Ashbaugh, H. S.; Vats, M.; Garde, S. Bridging Gaussian Density Fluctuations from Microscopic to Macroscopic Volumes: Applications to Non-Polar Solute Hydration Thermodynamics. *J. Phys. Chem. B* **2021**, *125*, 8152−8164.
(55) Remsing, R. C.; Patel, A. J. Water density fluctuations relevant to hydrophobic hydration are unaltered by attractions. *J. Chem. Phys.* **2015**, *142*, 024502.
(56) Rossky, P. J.; Zichi, D. A. Molecular librations and solvent orientational correlations in hydrophobic phenomena. *Faraday Symposia of the Chemical Society* **1982**, *17*, 69−78.
(57) Scaled-particle theory for hard spheres is entropic only, but for more realistic solutes, of interest here, our present expression is about the simplest available by including the enthalpic part, as far as we know.

https://doi.org/10.1021/acs.jpcb.2c02695
J. Phys. Chem. B XXXX, XXX, XXX−XXX